Erschienen in: Geochemistry, Geophysics, Geosystems ; 20 (2019), 6. - S. 2936-2954
https://dx.doi.org/10.1029/2019GC008312

Long-Term Impacts of the 1997–1998 Bleaching Event on the Growth and Resilience of Massive *Porites* Corals From the Central Red Sea

Juan P. D'Olivo[1,2], Lucy Georgiou[1,2], Jim Falter[1,2], Thomas M. DeCarlo[1,2,3], Xabier Irigoien[3,4,5], Christian R. Voolstra[3], Cornelia Roder[3,6], Julie Trotter[7], and Malcolm T. McCulloch[1,2]

[1]Oceans Graduate School, The University of Western Australia, Crawley, Western Australia, Australia, [2]ARC Centre of Excellence for Coral Reef Studies, The University of Western Australia, Crawley, Western Australia, Australia, [3]Red Sea Research Center, Biological and Environmental Sciences and Engineering Division, King Abdullah University of Science and Technology, Thuwal, Saudi Arabia, [4]AZTI - Marine Research, Spain, [5]IKERBASQUE, Basque Foundation for Science, Bilbao, Spain, [6]Alfred Wegener Institute Helmholtz Centre for Polar and Marine Research, Shelf Sea System Ecology, Helgoland, Germany, [7]School of Earth Sciences, The University of Western Australia, Crawley, Western Australia, Australia

Correspondence to:
J. P. D'Olivo,
juan.dolivocordero@uwa.edu.au

Abstract This study investigates the impact of extreme heat wave events on long-lived massive corals (*Porites* spp.) from the central Saudi Arabian Red Sea using trace element (Sr/Ca, Li/Mg, Mg/Ca, U/Ca, B/Ca, and Li/Ca) records preserved in the coral skeleton for the period between 1992 and 2012. Prior to 1998, the trace element records show strong correlations with sea surface temperature. However, during the prolonged high temperature phase associated with the 1998 El Niño event, the seasonal trace element signals were disrupted, which also coincided with a reduction in extension rates. This disruption in normally highly correlated seasonal trace element ratios-sea surface temperature relationships was unusually long, lasting for approximately 2 years in the inner-shelf reef site and nearly 4 years in the outer-shelf reef site. Although the seasonal signal of trace element ratios in both cores eventually stabilized, for the inner-shelf core the amplitude and absolute values in most trace element ratios remained significantly different compared to pre-1998 levels. This suggests that prolonged thermal stress can induce subtle but potentially long-lasting physiological changes that affect the elemental composition of the coral's calcifying fluid. The lack of indication of stress in the core records during later bleaching events (2003, 2005, and 2010) suggests that some of these physiological changes could have induced increased thermal tolerance, particularly for inner-shelf corals, lending support to the capacity for corals to acclimatize.

Plain Language Summary The future of coral reefs is jeopardized by global warming, particularly by marine heat waves and mass bleaching events, as evidenced by the 2016 and 2017 events. In this study the geochemical composition of the skeleton of two long-lived massive corals from the Red Sea was used to evaluate possible long-term acclimatization or changes in sensitivity to thermal stress. We detected a clear disturbance in the biomineralization process of the two corals following the 1998 bleaching event. However, posterior thermal stress events of similar magnitude were not registered in the skeletal growth or geochemical signature of the same corals hinting toward a possible long-term acclimatization following the exposure to the 1998 event.

1. Introduction

Discrete episodes of anomalously elevated temperature can severely affect the health of coral communities, even in areas exposed to naturally high temperatures (Schoepf et al., 2015). In the Red Sea, coral communities were severely affected by the 1997/1998 El Niño (DeVantier et al., 2000), which until the recent 2015/2016 El Niño was the most intense stress event in the region (Monroe et al., 2018). The 1997/1998 El Niño event began in the winter of 1997 and continued until the summer of 1998, causing prolonged periods of elevated sea surface temperature (SST) and mass coral bleaching worldwide. As a result, approximately 16% of reefs worldwide were destroyed by this single event alone (Wilkinson, 2000), with areas of the Red Sea experiencing up to 14-degree heating weeks (DHWs), well above the typical 4 DHW bleaching threshold (National Oceanic & Atmospheric Administration, 2000). Although in many places El Niño and La Niña result in opposing temperature trends (e.g., colder than average temperatures in response to La Niña and

warmer than average temperatures in response to El Niño), there are regions where both La Niña and El Niño can result in thermal anomalies of the same sign (positive or negative). In the summer of 2010, during the second strongest La Niña on record, corals of the Thuwal coastal region in the central eastern Red Sea experienced 9 to 11 DHWs of stress (Furby et al., 2013). This event resulted in mass coral bleaching followed by a drastic shift in coral community composition (Furby et al., 2013). Bleaching events not only result in the mass mortality of corals but also negatively affect the rates of calcification of the surviving individuals, threatening the future persistence of these unique ecosystems (Cantin & Lough, 2014; D'Olivo et al., 2013). Despite recent progress (T. M. DeCarlo et al., 2019; Gintert et al., 2018; Guest et al., 2012; Palmer, 2018; Pratchett et al., 2013; Putnam et al., 2017) not enough is known about the possible long-term adaptation or acclimatization of corals to thermal stress on the timescales relevant to global warming and how such adaptive responses could potentially improve the resistance of coral calcification, and thus the persistence of the coral reef framework, to climate change. Consequently, it is imperative that we develop a better understanding of how coral reefs will respond to periods of severe thermal stress as these events become more frequent and intense.

The skeletal geochemistry of long-lived massive corals such as *Porites* spp. has provided valuable information on both climate variability (Alibert & McCulloch, 1997; Beck et al., 1992; K. L. DeLong et al., 2007; Felis et al., 2000) and the response of coral calcification to these changes (Clarke et al., 2017; D'Olivo & McCulloch, 2017; Hetzinger et al., 2016). The translation of coral skeletal geochemistry into robust records of past climate has, however, been limited by an incomplete understanding of the mechanisms governing biogenic calcification and its influence on the incorporation of trace elements into the crystal lattice of the precipitated minerals (G. Gaetani & Cohen, 2006; Goreau, 1977; Sinclair & Risk, 2006). Thus, while the incorporation of trace elements like strontium (Sr) into the coral's aragonite skeleton is strongly correlated with SST, their partitioning can also be affected by a range of physiological processes or *vital effects* (Cohen et al., 2002; Marshall & McCulloch, 2002; Sinclair, 2005; Tanaka et al., 2015), particularly during periods of climate extremes and the associated physiological stress they cause. Although Sr/Ca, the most widely used coral paleothermometer, can be measured in the skeletons of massive corals with an analytical precision of better than 0.1% (Alibert & McCulloch, 1997; Beck et al., 1992; Kristine L. DeLong et al., 2013; Malcolm T. McCulloch et al., 1994; Moreau et al., 2015), its specific relationship with temperature for any given coral is still subject to physiological controls, which can become altered during periods of environmental stress. For example, Sr/Ca is typically inversely correlated to SST, but positive anomalies have been observed during periods of anomalously high temperature, such as those that occur during coral bleaching events (Hetzinger et al., 2016; Nurhati et al., 2009; Sagar et al., 2016). This disruption was originally associated with an inhibition of the enzyme (Ca^{2+} ATPase) that selectively affected the transport of Ca into the site of calcification (Marshall & McCulloch, 2002). Recent studies suggest that, in general, the common response of most trace element ratios to thermal stress appears to be a suppression of the typical temperature-driven seasonality (D'Olivo & McCulloch, 2017), even though the response of specific trace elements may exhibit different sensitivities to the degree of stress (D'Olivo & McCulloch, 2017). It is thought that thermal stress likely causes changes in calcifying fluid carbonate chemistry which then, in turn, alter the trace element composition of biomineralized calcium carbonate (Clarke et al., 2017; D'Olivo & McCulloch, 2017; T. M. DeCarlo & Cohen, 2017; Marshall & McCulloch, 2002).

Additionally, other geochemical temperature proxies, although not directly affected by the activity of the Ca^{2+}ATPase, still show disruptions following stress events (D'Olivo & McCulloch, 2017). For instance, it has been suggested that Mg^{2+} and Li^{+} are both transported to the site of calcification via the direct paracellular transport of ambient seawater before being incorporated into the aragonite crystal by similar physicochemical mechanisms that still remain the subject of active debate (Case et al., 2010; Paolo Montagna et al., 2014; Rollion-Bard & Blamart, 2015). While inorganic experiments suggest that Li^{+} is incorporated into aragonite through heterovalent substitution for Ca^{2+} (as opposed to homovalent substitution by Mg^{2+}; Hathorne et al., 2013; Marriott et al., 2004), other experimental and theoretical evidence suggests that both Li and Mg are incorporated through defects of the aragonite crystal (Paolo Montagna et al., 2014) and/or some other entrapment processes (Finch & Allison, 2008; Watson, 1996, 2004). Regardless of the specific mechanisms, differences in biogenic crystal growth mechanics appear to have little direct effect on the Li/Mg ratio in the coral skeleton, thus making this a relatively robust proxy for ambient seawater temperature that is essentially independent of vital effects (Marchitto et al., 2018; Paolo Montagna et al.,

2014; P. Montagna et al., 2009). The reliability of Li/Mg as a paleo-temperature proxy has been well validated for cold- and temperate-water corals (Case et al., 2010; Paolo Montagna et al., 2014; P. Montagna et al., 2009) but has received more limited use in corals living at higher (i.e., tropical) temperatures (D'Olivo et al., 2018; Fowell et al., 2016; Zinke et al., 2019). Nonetheless, the analysis of this proxy in tropical corals that have experienced periods of thermal stress has shown a clear disruption of the seasonal variability (D'Olivo & McCulloch, 2017). Interestingly, despite the very different mechanisms of incorporation for Sr/Ca and Li/Mg, the relationship between Sr/Ca and Li/Mg appears to remain constant even during periods of thermal stress, indicating that changes to the activity of the Ca^{2+}ATPase are not the sole driver of the anomalies in these elemental ratios.

Here we use a suite of trace element ratios (Sr/Ca, Mg/Ca, U/Ca, Li/Mg, B/Ca, and Li/Ca) to document the response of two massive *Porites* coral colonies from the inner shelf and outer shelf of the central eastern Red Sea to a strong cycle that occurred between 1997 and 2001. We first examine the impact of these events on the incorporation of trace elements into the aragonite lattice and then examine how thermal stress affects the relationships of these trace element ratios with SST. This is achieved by measuring each trace element at near monthly intervals for an ~18-year period starting from the year 1995 in the inner shelf, and for a ~21-year period in the outer shelf starting in 1992. The changes in trace element and skeletal growth are evaluated during multiple periods of elevated regional SSTs.

2. Materials and Methods

2.1. Site Description and Climatology

The Red Sea is a semienclosed water body roughly 2,000 km long and 200- to 300-km wide, where depths reach below 2,500 m in the central axis. It is highly saline (>39 ppm) due to low levels of rainfall in the surrounding region and limited exchange of water with rivers or other seas (Rasul et al., 2015). The Red Sea can be divided into three ecologically distinct regions: (1) the northern region that is connected to the Mediterranean Sea via the Suez Canal in the northwest and to the Gulf of Aqaba in the northeast; (2) the central region (20–24°N) that is extremely arid with minimal rainfall and riverine input, causing a nutrient poor environment; and (3) the southern region that is most heavily influenced by the Indian Ocean via exchange through the narrow Bab-al-Mandeb Strait (Rasul et al., 2015). SST in the southern part of the Red Sea is influenced by the incursion of Indian Ocean waters governed by the Asian monsoon system (and El Niño–Southern Oscillation [ENSO], Ionita et al., 2014; Klein et al., 1997), while the northern part is influenced by the North Atlantic Oscillation (NAO) and Arctic Oscillation (AO, Felis et al., 2000; Rimbu et al., 2001). Our work was conducted in the central region of the Red Sea, close to the coast of Saudi Arabia (around 22°N, Figure 1), which is mainly influenced by ENSO. The coastal area is composed of a narrow shelf ranging from 30 to 90 m in depth, which supports a complex set of reef systems and island features.

Daily local satellite SST data (1980–2013) derived from the Pathfinder Advanced Very High Resolution Radiometer (AVHRRv2) (Reynolds et al., 2007) were obtained online from the National Aeronautics and Space Administration THREDDS (v5.2) data server (http://thredds.jpl.nasa.gov/thredds/catalog_oceantemperature.html) at a spatial resolution of 0.25° × 0.25°. The King Abdullah University of Science and Technology obtained daily resolution in situ SST data from loggers fixed at the inner-shelf and outer-shelf reef sites from September 2012 to September 2013 (Figure S1 in the supporting information, Roik et al., 2015; Roik et al., 2016). Comparisons between the two data sets indicates a general good agreement between the satellite and in situ temperature with the AVHRR temperatures being approximately 0.5 °C colder compared to the in situ temperatures recorded in the outer-shelf reef (Figure S1). SSTs in the central Red Sea range from around 25 °C in February to 31 °C in September, with strong diurnal variability around reef platforms (Davis et al., 2011; Reynolds et al., 2007). Wave exposed areas of reefs can typically vary by 0.5 to 1.5 °C, while the wave protected side of the same reef will experience changes of 2 to 5 °C over the same diurnal period (Davis et al., 2011). Spatial temperature variability on reefs in the central Red Sea has been attributed to a combination of regional climate forcing, such as wind-driven cooling, wave-driven circulation, and large-scale buoyancy-driven circulation (Davis et al., 2011; Monismith et al., 2006).

DHWs, a measure of the accumulation of thermal stress over a period of 12 weeks, were calculated using the AVHRRv2 daily data based on the methodology described by the National Oceanic and Atmospheric

Figure 1. Study site in the central Red Sea highlighting the two sampled reefs. Red Box represents locality of sampling area (insert), stars indicate the locations of the reef sites where the *Porites* coral cores were retrieved: Abu Shosha (inner shelf) and Shi'b Nazar (outer shelf).

Administration Coral Reef Watch website (https://coralreefwatch.noaa.gov/satellite/methodology/methodology.php). Briefly, DHWs were calculated as the accumulation of HotSpots over a 12-week window, where the coral bleaching HotSpot product highlights SST values greater than 1.0 °C above the maximum monthly mean (MMM) SST. The maximum monthly mean was calculated for the reference period of 1985 to 1993 (excluding 1991 and 1992) according the National Oceanic and Atmospheric Administration Coral Reef Watch methodology (Figure 2).

The 1997/1998 El Niño was associated with a worldwide bleaching event, although the three regions of the Red Sea were not affected equally by this event. No bleaching was observed in the northern region of the Red Sea due to the cooler conditions and notable upwelling in the region (DeVantier et al., 2000). However, severe bleaching was documented in the southern region of the Red Sea, particularly around the central Saudi Arabian coast (DeVantier et al., 2000; Rasul et al., 2015). Here ~14 DHWs were experienced during the summer of 1998, with seawater temperatures that were ~1.3 °C higher than normal from the summer of 1997 to the summer of 1998 (AVHRR v5.2, Figure 2; W. Liu et al., 2015). Given that widespread bleaching and mortality is likely to occur at around eight DHWs (G. Liu et al., 2013), this created a thermally stressful environment for shallow-water corals, which periodically experienced temperatures that were > 1 °C above the MMM (Figure 2). Following the 1997/1998 El Niño event, summer SST anomalies remained above the MMM during five of the next seven years (1999, 2001, 2002, 2003, and 2005). In addition to the episodic El Niño related events, the Red Sea's average SST is increasing at a faster rate than most tropical regions, with models forecasting a 2 to 3 °C SST rise in the central Red Sea by the end of the 21st century (Cantin et al., 2010; Monroe et al., 2018; Stocker et al., 2013).

2.2. Coral Core Sampling

Coral cores were collected near Thuwal in the central Red Sea from two sites: Abu Shosha on the inner shelf (~5 km from shore, 6.6-m depth, 39°02′59.7″E, 22°18′13.1″N) and Shi'b Nazar on the outer shelf (~25 km from shore, 5-m depth: 38°53′55.99″E, 22°22′20.12″N) (Fig. 1). Core samples (5 cm in diameter and up to 50 cm in length) were taken in April 2013 from living massive colonies of *Porites lutea* (RED4; outer shelf) and *Porites australiensis* (RED2; inner shelf) identified based on corallite structure following Veron (2000). Cores were first cleaned with fresh water and then dried and packed for transport to the University of Western Australia for processing and analysis. The cores were cut into slices 6- to 7-mm thick along the length of the core using an automatic core cutter fitted with a diamond blade. The resulting slices were bleached overnight in a 1:1 NaClO solution before being washed thoroughly in deionized water, ultrasonicated 3 times, and dried at ~50 °C in a laboratory oven. A set of slices from the middle of each coral core was

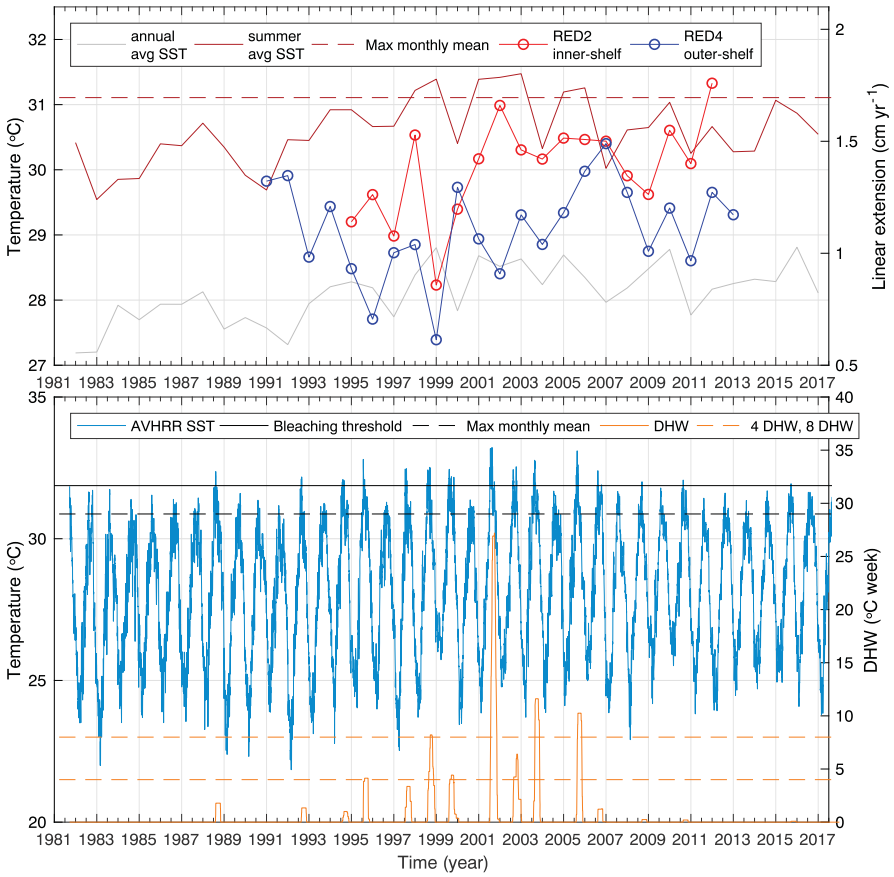

Figure 2. Records of temperature and linear extension. (top) Annual records of coral linear extension for cores inner-shelf RED2 and outer-shelf RED4, compared to summer (July–September) average temperature and annual (January–December) average temperature near Thuwal. (bottom) High-resolution daily sea surface temperature AVHRRv2 data near Thuwal and corresponding degree heating weeks. DHWs = degree heating weeks; AVHRRv2 = Advanced Very High Resolution Radiometer.

taken for X-radiography, and digital images were obtained using Clarity Pacs (jCRco) software. Profiles of optical density along each core were digitized and extracted using the software CoralXDS (Ver 4.6, NOVA Southeastern University). Powder samples were taken at 1.25-mm intervals for both cores with a computer controlled Zenbot drill. This sampling strategy resolved 10 to 11 samples per year for the outer-shelf core and 12 to 13 samples per year for the inner-shelf core during years unaffected by temperature anomalies. Samples were collected along the axis of growth established from the X-radiographies following the directions of the corallites.

2.3. Geochemical Analysis

Powdered coral samples were processed in the Advanced Geochemical Facility for Indian Ocean Research Clean Laboratory based at University of Western Australia following established methods (D'Olivo et al., 2018; Holcomb et al., 2015). All sample and standard solutions were prepared using subboiling distilled HNO_3 (Savillex DST-1000) and 18.2 MΩ water (Millipore). Coral powder samples were weighed (10 ± 0.2 mg) and dissolved in 0.5 M HNO_3 before being centrifuged. An aliquot of 31 µL was pipetted into 2.97 mL of 2% HNO_3 (≡ 100 ppm Ca for B, Li, and Mg analysis) and further diluted to 10 ppm Ca using 2% HNO_3 spiked solution containing 0.095 ppb Bi, 0.19 ppb Pr, ~19 ppb Sc, and 19 ppb Y (to correct for variable instrumental mass bias) for Ca, Mg, Sr, and U analysis (Holcomb et al., 2015). One aliquot of the JCp-1 coral standard was processed along with every 30 samples in order to assess the quality and reproducibility of our full chemical treatment.

2.4. Analytical Procedure

Trace element measurements were carried out on a Thermo Fisher Scientific (Bremen, Germany) X Series II quadrupole inductively coupled plasma mass spectrometer using the standard Xt interface with the plasma screen fitted. The sample introduction system consisted of an autosampler (Elemental Scientific SC4 DX) attached to a self-aspirating Teflon microflow nebulizer (Elemental Scientific PFA-ST) using a 100 μL/min capillary fitted to a quartz spray chamber cooled to 2 °C (Elemental Scientific PC3). All analyses were then carried out in peak-hopping pulse counting mode; washout and uptake times were 20 and 100 s per sample, respectively. Typical sensitivity of the instrument was ~300–500 kcps for ^{43}Ca aspirating a solution containing 10-ppm Ca. For the determination of Li/Mg and B/Ca, ^{7}Li, ^{11}B, and ^{25}Mg were acquired in 100 sweeps and 6 repetitions for a total acquisition time of 112 s per sample ([Ca] = 100 ppm). ^{25}Mg, ^{43}Ca, ^{86}Sr, and ^{238}U were acquired for the determination of metal to Ca ratios in 100 sweeps and 8 repetitions for a total acquisition time of 224 s per sample ([Ca] = 10 ppm). Long-term reproducibility (representative of ~1 year of data collection) of Me/Ca derived from repeated analyses of individual aliquots of the JCp-1 coral powder is as follows: Li/Mg = 1.5%, B/Mg = 8.7%, Mg/Ca = 0.9%, Sr/Ca = 0.4%, and U/Ca = 1.2% (2 s Relative Standard Deviation; n = 17, D'Olivo et al., 2018). These uncertainties are assumed to be representative for individual analysis of sample powders and are comparable to the interlaboratory precisions defined by Hathorne et al. (2013). The B/Ca data were estimated from combining B/Mg and Mg/Ca data, while Li/Ca was estimated by combining the Li/Mg with Mg/Ca data. The reliability of these procedures has been further confirmed by occasional repeat analyses of sample powders.

2.5. Coral Chronology and Skeletal Growth Parameters

An initial chronology was ascertained from X-radiograph images based on visual inspection of the annual high- and low-density band patterns (Figure 3). Establishing the chronology from X-ray images was particularly challenging in these cores due to double banding and density band changes associated with the cessation or slow growth occurring in late 1998 to 1999. Distinct fluorescent lines formed by river runoff events, which provide chronological markers in other systems (D'Olivo et al., 2013; Isdale, 1984), are absent in corals from this region; however, faint annual luminescent bands assisted assigning a chronology. Slices were cut along the axis of maximum growth to expose the most appropriate surface for geochemical sampling as identified from the X-ray images. Breaks and fissures along the core were avoided to provide the most homogenous sampling areas.

The final age model was assigned using AnalySeries (Paillard et al., 1996) by fixing the timing of maxima (minima) in Sr/Ca and Li/Mg ratios to the known timing of minima (maxima) in SST records and interpolating the resulting chronologically fixed trace element time series at near monthly resolution. Both Sr/Ca and Li/Mg were checked synchronously to maximizing the correlation of both trace element ratios with the SST time series, based on the built-in correlation function included in AnalySeries (K. L. DeLong et al., 2007). Linear extension rates were then calculated using the trace element chronology and the sampling distance.

Development of the chronology during 1997/1998 proved especially challenging due to anomalies in the geochemical signal during, and for up to ~ 4 years after, the ENSO event. As with the full chronology, we made an initial estimate of the location of the 1997/1998 event within each core based on visual inspection of annual density banding in the X-ray images, counting high/low density band pairs downward from the top of the core. We then confirmed that the apparent 1997/1998 density bands corresponded to the faint luminescence bands (Figure S2). Our monthly linear extension rates (based on the apparent timing of element/Ca ratios) were also used to assess the growth rates implied by our 1997/1998 chronology. For example, if our initial chronology were missing a full year between 1998 and 2000, then linear extension during this time would have been 60% higher than that during the rest of the record. Finally, we independently evaluated monthly linear extension rates using dissepiments, thin sheets of skeleton located at the base of the tissue layer that are accreted once per lunar cycle (~29.4 days) (Barnes & Lough, 1993; T. M. DeCarlo & Cohen, 2017). We prepared petrographic thin sections of the skeleton corresponding to approximately 1998–2000, constructed photomosaics of the thin sections with a ScanScope XT digital slide scanner using 20X magnification, traced the dissepiments visible in the compiled images, and measured the distance between them following the procedures described in T. M. DeCarlo and Cohen (2017).

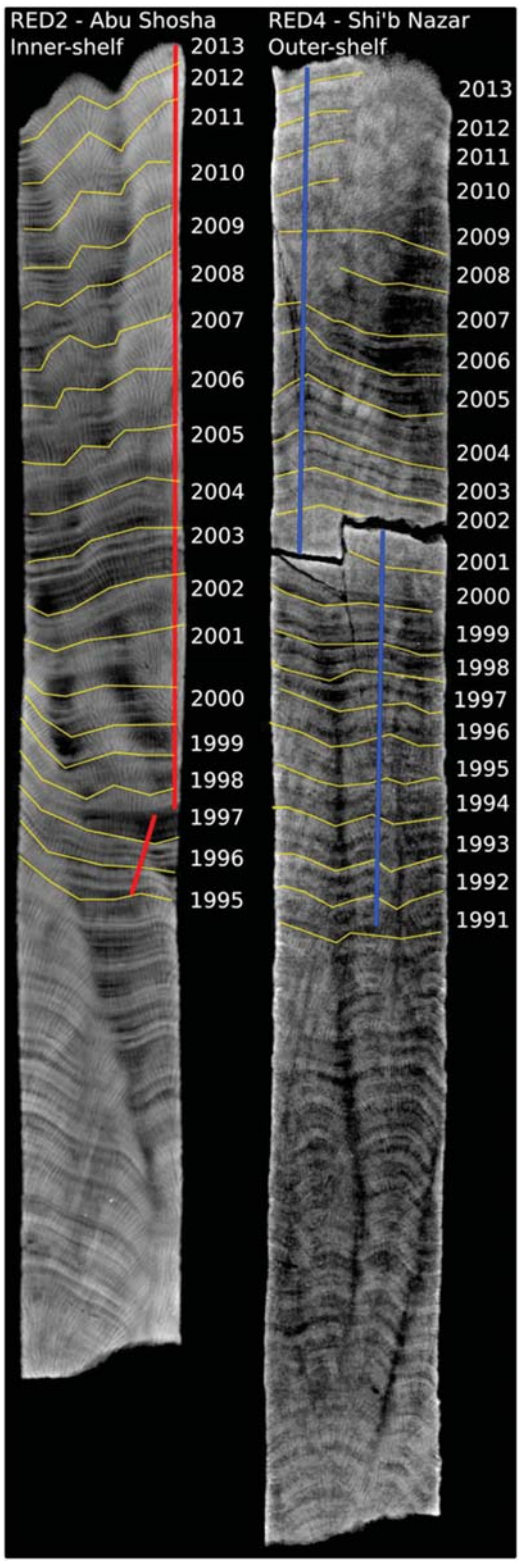

Figure 3. Annual density bands in two coral cores from the central Red Sea revealed by X-Ray radiographs. Annual density band chronology highlighted by yellow lines. The red and blue lines highlight the sample paths followed for the geochemical analyses.

U series dating (M. T. McCulloch & Mortimer, 2008) was applied on coral core samples from both the inner and outer reef locations in an attempt to independently constrain the start and end dates of the anomalous trace element patterns observed in these cores during the late 1990s. From each core a sample of ~200 mg was dated prior to the commencement of the anomalous period, with a second reference sample dated from the younger upper portion of the core whose age was clearly constrained from the density bands and trace element seasonality. The purpose of the reference samples (February 2006 for the inner core and February 2003 for the outer core) was to provide constraints on the initial $^{230}Th/^{232}Th$ ratio whose value is critical to obtaining accurate age estimates at subannual resolution (M. T. McCulloch & Mortimer, 2008). The uncertainty associated with these corrections is however still significant (see Table S1), being equivalent to ~2 years in this region.

2.6. Statistical Analysis

The most recent (from the top of the core) measurements back to 2012 were omitted from any statistical analysis as these include residue from the coral tissue layer (D'Olivo et al., 2018). The response of a variable to a predictor was assessed using robust regressions, with weighted linear regressions employing bisquare-weighting function. The location of abrupt changes in the trace element signal was detected using a parametric global change-point function based on the mean. One change point was allowed for the inner-shelf data, while two change points were allowed for the outer-shelf data, as this provided the best fit with the data (see supporting information). Analyses of covariance (ANCOVA) were performed to test if the relationship between different elemental ratios changed over time. For this test, the data were divided into three groups: prior to 1998, 1998 to 2001, and post-2001; and the relationship between all the combinations of trace element ratios was compared. All statistical analyses (regressions, change point, and ANCOVA) were performed using Matlab version R2017b.

3. Results

The annual average AVHRR SST data suggested the waters near Thuwal in the central Red Sea have experienced an increase of ~0.6 °C from the 1980s to the present (Figure 2). Average summer temperatures (July to September) were highest between 1998 and 2005, with 2001 corresponding to the warmest summer on record (1981 to 2017). Average summer temperatures in 1998, 1999, 2001, 2002, 2003, and 2005 were higher than 1 SD of the historical (1981 to 2017) average summer values. The DHW metric suggested recurrent events of high thermal stress between 1995 and 2005, with more than 4 °C weeks in 1995, 1999, and 2002; and more than 8 °C weeks in 1998, 2001, 2003, and 2005.

Monthly records of trace elements (Li/Mg, Li/Ca, B/Ca, Mg/Ca, Sr/Ca, and U/Ca) showed clear seasonal variations in both cores RED2 (inner shelf, Figure 4) and RED4 (outer shelf, Figure 5). However, the geochemical signals of both cores were characterized by abrupt changes in mean values and periods in which the seasonal amplitude was reduced or disappeared in most trace element ratios. In both coral records, there was a disruption in the geochemical seasonal signal of all trace element ratios in the late 1990s. The duration and pattern of this disruption, however, varied between the two cores and between trace element ratios.

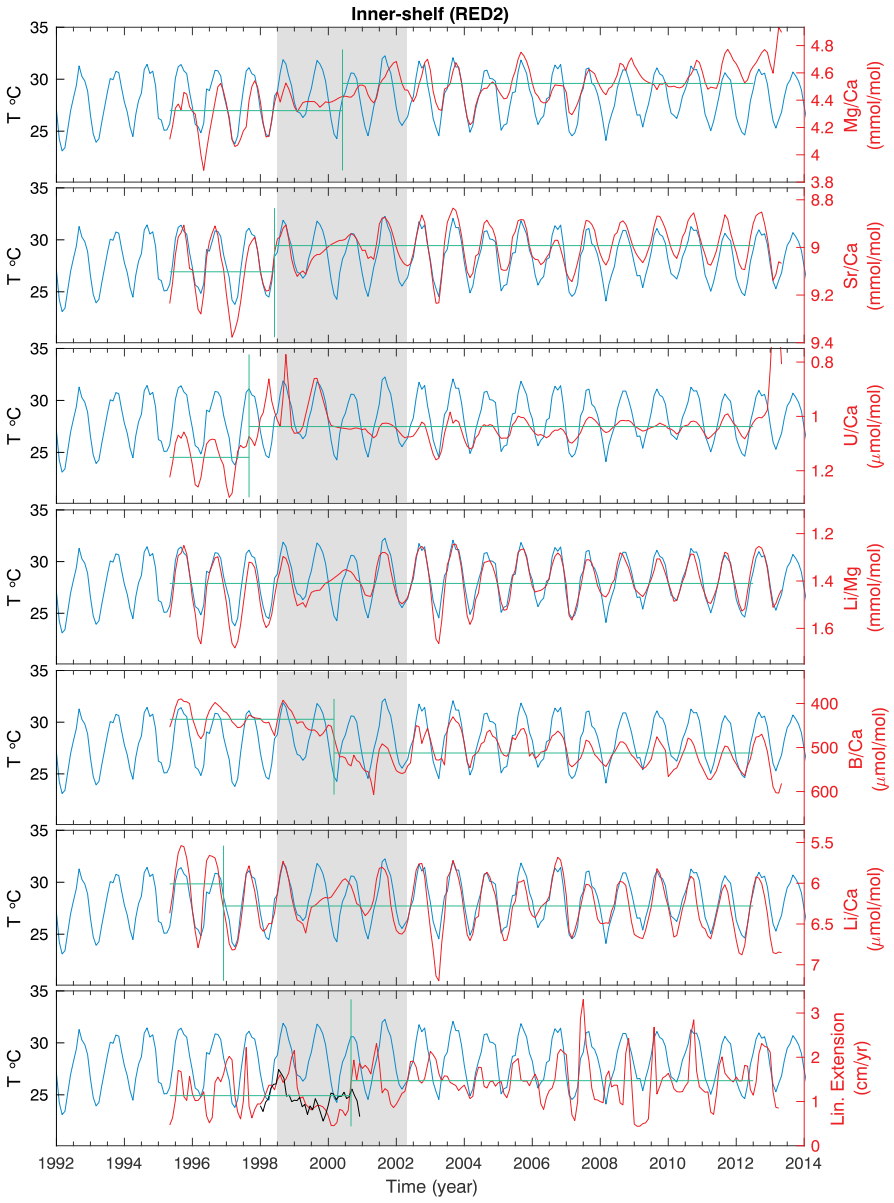

Figure 4. Monthly records for coral trace element ratios and linear extension (red) for the inner-shelf core from Abu Shosa Reef in the central Red Sea compared to AVHRR SSTv2 data (light blue). Also included is near monthly linear extension estimated from the dissepiment data over 1998–2000 (black). Detected change points (vertical green line) and mean values for the data included between each change point (horizontal green line). Gray shaded area highlights the period of maximum stress detected in inner-shelf and outer-shelf (see Figure 5) geochemical records. AVHRR = Advanced Very High Resolution Radiometer; SST = sea surface temperature.

Coinciding with this disruption, annual linear extension reconstructed from the geochemical age model recorded minimum values in 1999 for both cores.

3.1. Difference Between Inner-Shelf and Outer-Shelf Sites

The *Porites australiensis* inner-shelf core showed a disruption in the seasonality for Mg/Ca, U/Ca, and B/Ca starting around 1998, whereas for Sr/Ca, Li/Mg, and Li/Ca the disruption was only clear a year later (1999), with all trace element ratios recovering a clear seasonality by 2002 (Figure 4). Despite the recovery of seasonality by 2002, change-point analysis suggests that changes in the mean values of Mg/Ca, Sr/Ca,

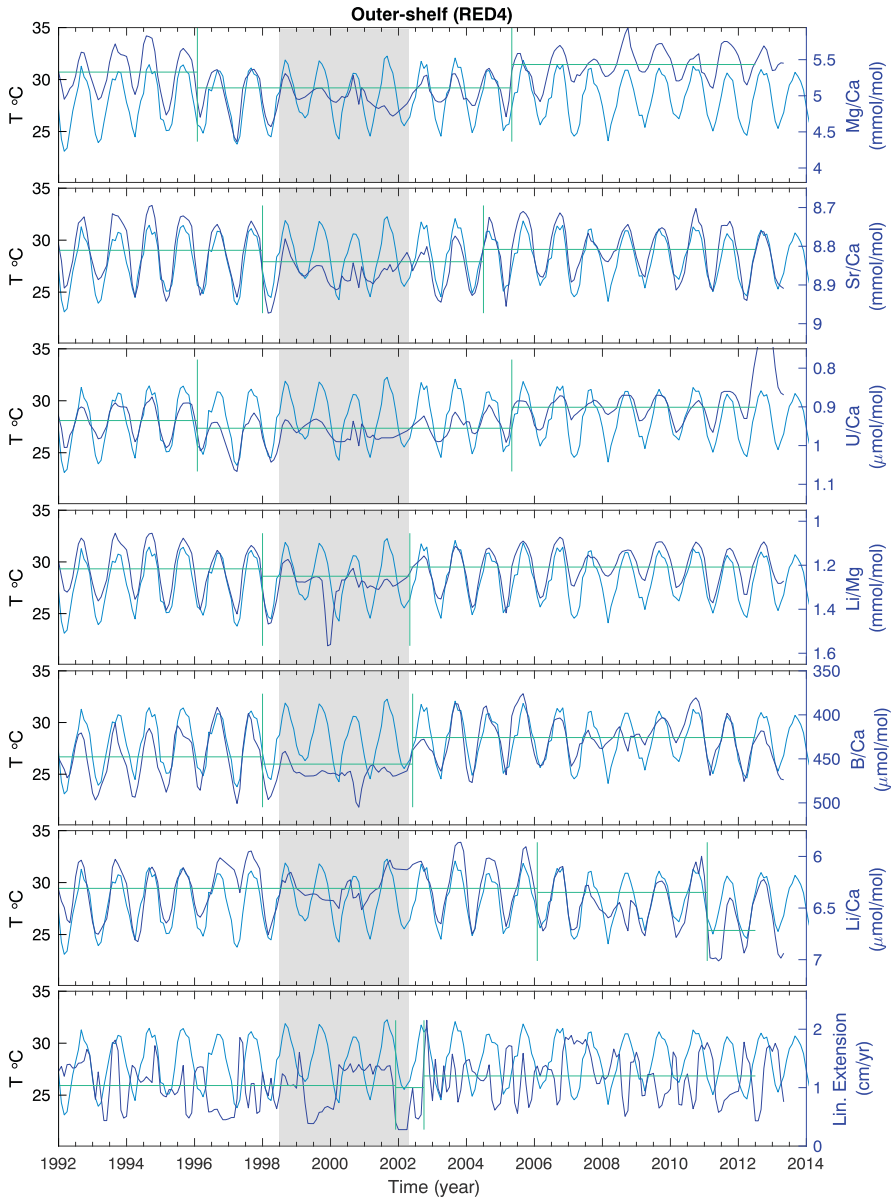

Figure 5. Monthly records for coral trace element ratios and linear extension (dark blue) for the outer-shelf core from Shi'b Nazar Reef in the central Red Sea compared to AVHRR SSTv2 data (light blue). Up to two detected change points (vertical green line) and mean values for the data included between each change point (horizontal green line). Gray shaded area highlights the period of maximum stress detected in inner-shelf (see Figure 4) and outer-shelf geochemical records. AVHRR = Advanced Very High Resolution Radiometer; SST = sea surface temperature.

U/Ca, B/Ca, and Li/Ca occurred as a result of this disturbance (Figure 4). Comparison of the relationship between the different elemental ratios prior to 1998, during the stress events (1998 to 2001) and after recovery (post 2001), highlights two main patterns. The elemental ratios Mg/Ca, Sr/Ca, Li/Mg, and Li/Ca appear to maintain similar relationships over the whole length of the records (Table 1). In comparison, U/Ca and B/Ca show a breakdown of the relationship with other elements between 1998 and 2001, and a markedly different relationship post-2001, compared to pre-1998. The ANCOVA indicated that the relationships of U/Ca and B/Ca with the other trace element ratios changed significantly in slopes between the three periods, while the relationship between the other elements remained essentially unchanged (Table 2).

Table 1
Correlations Coefficients and Significance for the Relationship Between the Different Trace Element Ratios for Porites spp. Coral Core RED2 From the Inner-Shelf Reef Abu Shosha (Top) and Core RED4 From the Outer-Shelf Reef Shi'b Nazar (Bottom)

		Sr/Ca		U/Ca		Li/Mg		B/Ca		Li/Ca	
Period		*r*	*p*	*r*	*p*	*r*	*p*	*r*	*p*	*r*	*p*
Inner shelf (RED2)											
Pre-1998	Mg/Ca	−0.684	0.000	−0.149	0.373	−0.732	0.000	−0.619	0.000	−0.393	0.015
1998–2001		−0.701	0.000	0.054	0.738	−0.571	0.000	0.275	0.082	−0.275	0.082
Post-2001		−0.660	0.000	−0.770	0.000	−0.655	0.000	−0.279	0.002	−0.348	0.000
Pre-1998	Sr/Ca			0.436	0.006	0.953	0.000	0.690	0.000	0.880	0.000
1998–2001				0.046	0.774	0.947	0.000	−0.144	0.370	0.820	0.000
Post-2001				0.898	0.000	0.931	0.000	0.636	0.000	0.836	0.000
Pre-1998	U/Ca					0.254	0.124	0.107	0.522	0.268	0.104
1998–2001						0.064	0.690	0.543	0.000	0.132	0.412
Post-2001						0.849	0.000	0.446	0.000	0.688	0.000
Pre-1998	Li/Mg							0.821	0.000	0.914	0.000
1998–2001								−0.003	0.983	0.935	0.000
Post-2001								0.754	0.000	0.930	0.000
Pre-1998	B/Ca									0.737	0.000
1998–2001										0.099	0.536
Post-2001										0.799	0.000
Outer shelf (RED4)											
Pre-1998	Mg/Ca	−0.907	0.000	−0.976	0.000	−0.938	0.000	−0.700	0.000	−0.468	0.000
1998–2001		−0.591	0.000	−0.758	0.000	−0.419	0.006	−0.263	0.097	0.222	0.162
Post-2001		−0.745	0.000	−0.854	0.000	−0.755	0.000	−0.597	0.000	−0.095	0.290
Pre-1998	Sr/Ca			0.898	0.000	0.986	0.000	0.856	0.000	0.772	0.000
1998–2001				0.706	0.000	0.632	0.000	0.518	0.001	0.496	0.001
Post-2001				0.719	0.000	0.929	0.000	0.790	0.000	0.522	0.000
Pre-1998	U/Ca					0.922	0.000	0.659	0.000	0.467	0.000
1998–2001						0.363	0.020	0.290	0.066	−0.058	0.719
Post-2001						0.727	0.000	0.516	0.000	0.198	0.026
Pre-1998	Li/Mg							0.844	0.000	0.741	0.000
1998–2001								0.231	0.146	0.433	0.005
Post-2001								0.821	0.000	0.591	0.000
Pre-1998	B/Ca									0.799	0.000
1998–2001										0.426	0.005
Post-2001										0.602	0.000

Note. Trace element ratios divided into time intervals, pre-1998 ENSO years, post-2001, and ENSO affected years (1998–2001). Lack of significant relationship ($p > 0.05$) is highlighted in red. ENSO = El Niño–Southern Oscillation.

The *Porites lutea* outer-shelf coral also showed a disruption in the seasonality of all trace elements starting around 1998 (Figure 5), with the timing for the onset of this disruption less clear in Mg/Ca, U/Ca, and Li/Ca, possibly starting in 1996. For similar reasons, the exact timing of the recovery is not definitive. The change-point analysis suggests a change in the mean of most elements occurred between 1996 and 2005, but the disruption in the seasonality appears more evident between 1998 and 2001. Compared to the inner-shelf core, the outer-shelf showed no consistent change in the relationship between the different trace element ratios. The ANCOVA showed a significant change in the slope of the relationships of Li/Mg with Sr/Ca, B/Ca, and Li/Ca between the three periods (pre-1998, 1998 to 2001, and post-2001; Table 2).

3.2. Chronology During 1998 to 2001

Establishing the chronology of the coral records during the period of stress (~1998 to 2001) was particularly challenging due to the lack of seasonality in the geochemical proxies. Our determinations of ages using U-Th

Table 2
ANCOVA Results Comparing the Relationships Between the Different Trace Element Ratios (TER) During the Three Periods (Pre-1998, 1998 to 2001, and Post-2001)

TER	Sr/Ca	U/Ca	Li/Mg	B/Ca	Li/Ca
Inner shelf - Abu Shosha (RED2)					
Mg/Ca	0.875	*0.000*	0.705	*0.000*	0.911
Sr/Ca		*0.000*	0.565	*0.000*	0.201
U/Ca			*0.000*	0.051	*0.000*
Li/Mg				*0.000*	0.066
B/Ca					*0.000*
Outer shelf - Shi'b Nazar (RED4)					
Mg/Ca	0.431	0.178	0.054	0.339	0.080
Sr/Ca		0.094	*0.001*	0.126	0.895
U/Ca			0.229	0.172	0.643
Li/Mg				*0.000*	*0.004*
B/Ca					0.978

Note. Differences in the slopes for the relationship between trace element ratios over different periods are significant in cases of $p < 0.05$ (highlighted in italics). ANCOVA = analyses of covariance.

dating indicated the disruption lasted 6 ± 2 years for the outer-shelf coral (Shi'b Nazar) and 2 ± 2 years for the inner reef sample (Abu Shosha), thus the analytical uncertainties associated in estimating the initial $^{230}Th/^{232}Th$ are too large to accurately constrain the duration of the event. To better resolve the chronology during this period, we relied on the information from the annual density bands and luminescent bands, which was independently confirmed by dissepiment counts. The dissepiments of the inner-shelf coral (RED2) in the section identified as 1998 to 2000 from the density and luminescent bands were particularly clear (Figures 3 and S2). The 3 years of growth identified based on the density and luminescent bands closely coincided with the 42 dissepiments identified over the same period (3.3 years, based on ~12.4 dissepiments per year; Figure S3). Furthermore, a clear reduction in the distance between dissepiments for the year 1999 confirms the estimates of reduced linear extension during this year based on the geochemical age model (i.e., the timing between each 1.25-mm subsample, Figure 2). Between 1998 and 2000, the average dissepiment-based linear extension (1.06 mm per lunar month or 1.3 cm per year) is similar to that derived from the element ratios (1.2 cm per year), which clearly demonstrates the validity of our chronology. The dissepiments in coral RED4 (outer shelf) formed *blistering* patterns in which dissepiments connect to each other (see Barnes & Lough, 1993), precluding their use for developing a chronology (Figure S4). Additionally, the luminescent bands were less clear, preventing us from confirming the age model obtained based on density bands for this coral. However, in total, the agreement between the density bands, the U-Th dating, and the partial seasonality observed for Sr/Ca and Mg/Ca during this period provides confidence in our age model.

4. Discussion

Summer SST anomalies and DHW highlight a decade of unprecedented warm temperatures from 1995 to 2005 near Thuwal, in the central Red Sea (Figure 2). During this period, summer temperatures exceeded the nominal bleaching threshold in multiple years (6 out of 11) indicating that the corals in this region were exposed to repeated thermal stress events. The earliest reports of coral bleaching for the region correspond to 1998 with 30% mortality reported around Rabigh, ~40-km north of our study site (DeVantier et al., 2000; Osman et al., 2018). This extended period of stress was reflected in the two coral cores studied here and presented itself as a reduction in linear extension and a major disruption in seasonality in all trace element ratios during or immediately after 1998 and lasting for 2 to 4 years (Figures 4 and 5). Disruption of coral geochemical signal in response to thermal stress has previously been documented but typically lasted only a few months (Clarke et al., 2017; D'Olivo & McCulloch, 2017; T. M. DeCarlo & Cohen, 2017; Hetzinger et al., 2016; Marshall & McCulloch, 2002; Sagar et al., 2016; Suzuki et al., 2003). While the duration of the effects of thermal stress reported here is uncommonly long, there is at least one other study that documented trace element disruptions associated with the 1998 event lasting up to 5 years in a coral from the Japanese Islands of Ogasawara in the western North Pacific Ocean (Felis et al., 2009). Similarly, growth in *Porites* sp. from the inner Great Barrier Reef took 3 to 4 years to return to pre-ENSO El Niño rates (Cantin & Lough, 2014; D'Olivo et al., 2013). The effect of the 1997/1998 El Niño-instigated warming event on trace element ratios has also been documented in coral core records from other locations, such as the Lakshadweep Archipelago in the Indian Ocean and the Arabian Sea, where trace element seasonality recovered over annual timescales (Nurhati et al., 2009; Sagar et al., 2016).

Though the high correlations between most trace element ratios and SST returned after 3 to 4 years following the breakdown at both shelf sites, they were generally more robust on the outer-shelf than on the inner-shelf core (Figures 6 and 7 and Table 1). This was especially true for the Li/Mg-SST correlation as in both cores it returned to the same level as prior to the 1997–2001 phase of the ENSO cycle. By 2004, the relationship between Sr/Ca and SST in the outer-shelf core also returned to levels prior to the ENSO cycle of 1997–2001, despite erroneous indications of cooling (equivalent to ~6 °C) during the thermal stress period. Additionally, Sr/Ca showed a mean change of >0.08 mmol/mol (equivalent to ~2 °C) for the inner shelf

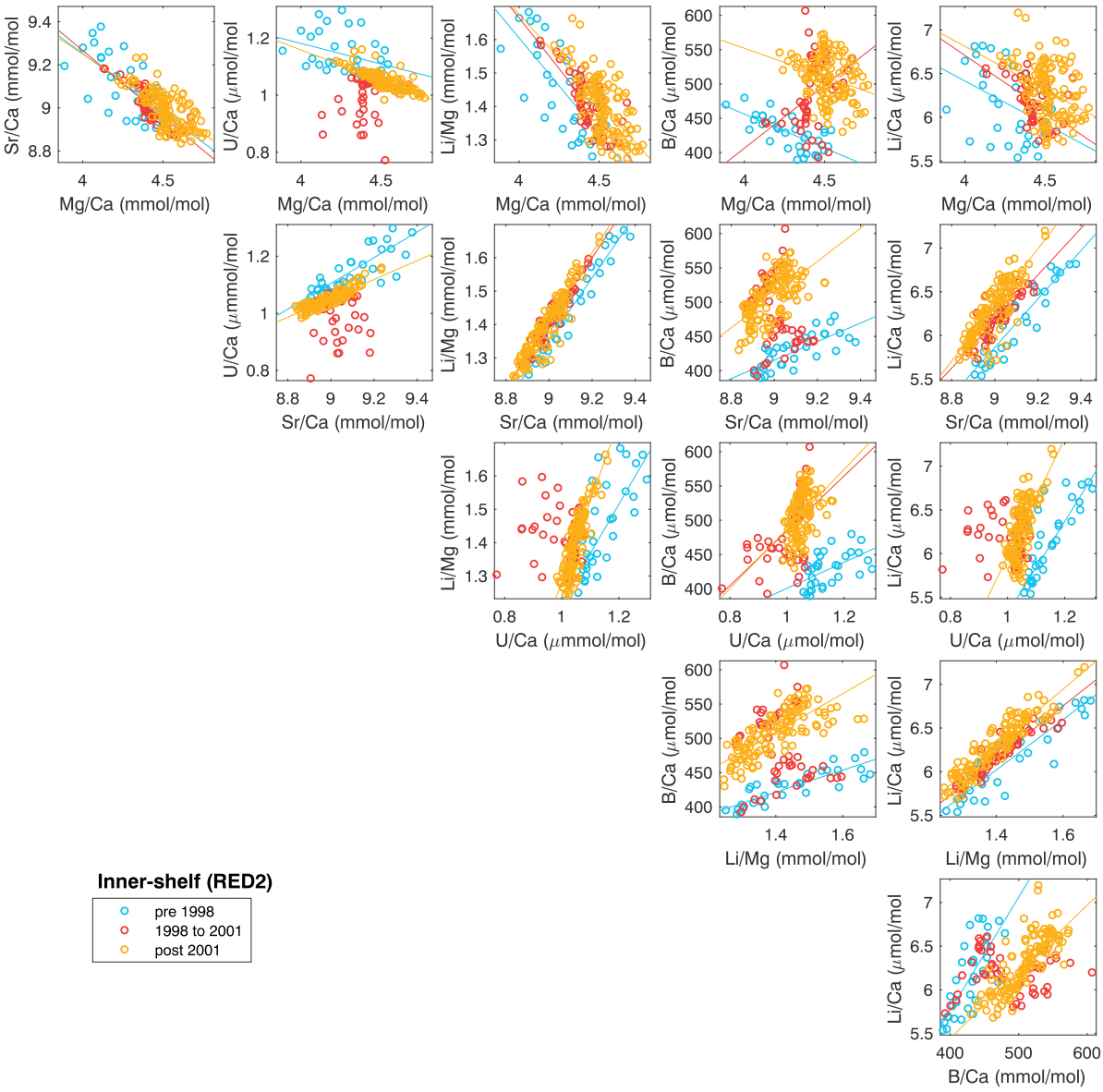

Figure 6. Trace element relationships for the inner-shelf core RED2. Scatterplots showing the relationships between the different trace element ratios pre-1998, between 1998 and 2001, and post-2001 for the inner-shelf core RED2 from Abu Shosha. Also included are the robust linear regressions when significant ($p < 0.05$).

after the stress event compared (Figure 8). The differences in trace element patterns recorded between the inner and outer reef sites are indicative of physiological changes that affect the mechanism by which trace elements are incorporated into the coral skeleton. Disruptions to temperature-sensitive element ratios (e.g., Sr/Ca) during and after peak temperatures cast doubt on their ability to accurately reconstruct such high-temperature events in paleo records. The data here further support the notion that coral physiology strongly influences the geochemical composition of the skeleton, including single element/Ca ratios like Sr/Ca. Our finding that Li/Mg was the most robust proxy of seawater temperature measured in corals from both the inner and outer shelfs further reinforces the role that the dynamics of Ca^{2+} transport and/or Rayleigh fractionation plays in controlling the reliability of trace element/Ca-based thermometry. We also note that the shifts in interannual mean Sr/Ca during and after the stress period are mirrored by U/Ca, consistent with predictions that U/Ca tracks the nontemperature physiological effects imparted by the coral on Sr/Ca (Thomas. M. DeCarlo et al., 2016). Therefore, alternative temperature proxies, such as

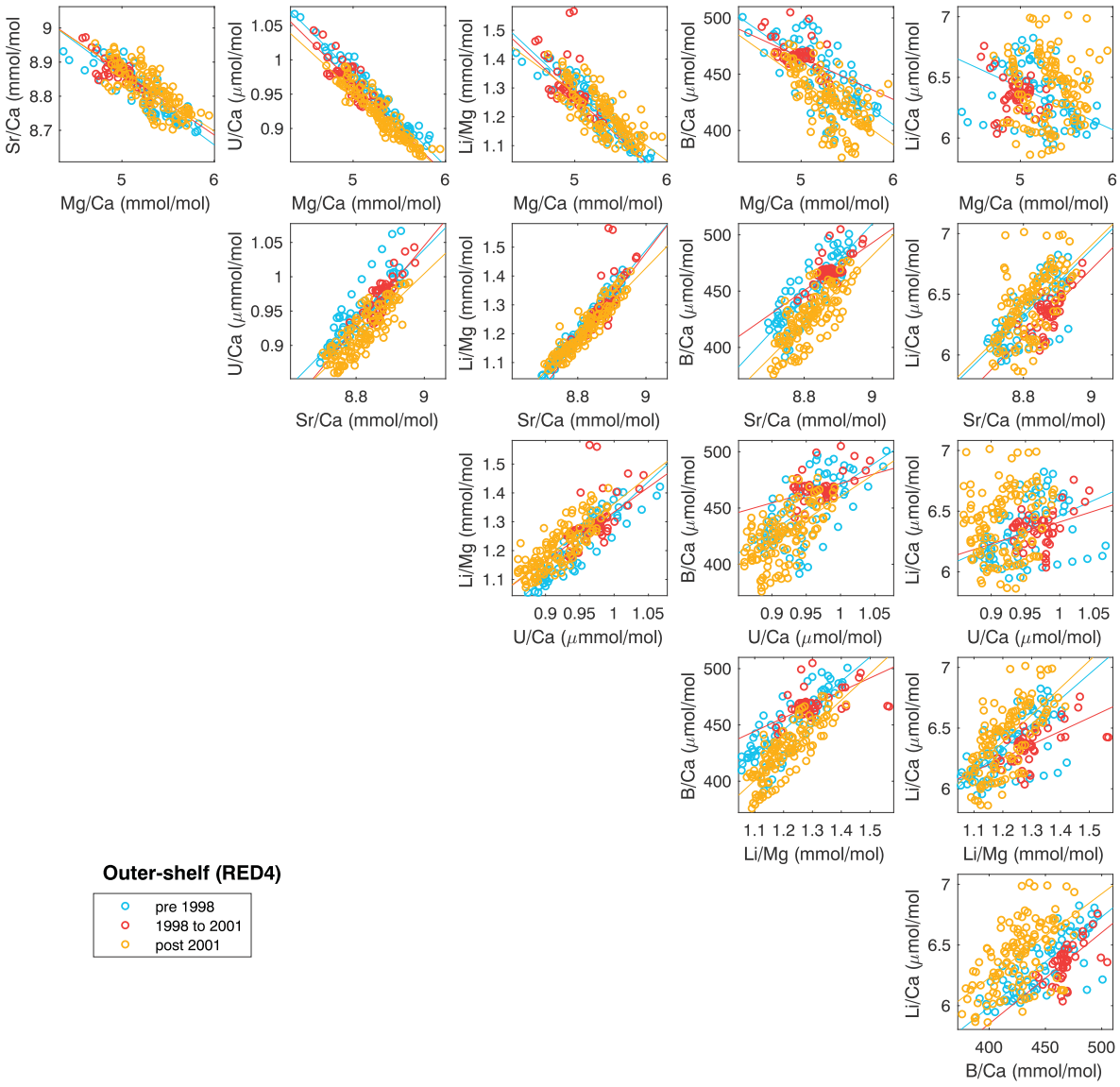

Figure 7. Trace element relationships for the outer-shelf core RED4. Scatterplots showing the relationships between the different trace element ratios pre-1998, between 1998 and 2001, and post-2001 for the outer-shelf core RED4 from Shi'b-Nazar. Also included are the robust linear regressions when significant ($p < 0.05$).

those recently proposed based on Li/Mg (Paolo Montagna et al., 2014) and Sr-U (Thomas. M. DeCarlo et al., 2016), may be more reliable over a wider range of climatic conditions.

The major disruption in trace element-SST relationships observed in the Red Sea *Porites* corals coincided with, and was clearly initiated by, the intense 1997/1998 ENSO cycle, but the reason the disturbance lasted 2 to 4 years is less certain. It may have been a result of additional regional thermal stress associated with the strong ensuing La Niña which, in this case, also caused an extended period of elevated ocean temperatures and consequent mass coral bleaching in other regions (Zinke et al., 2015). Although there are no records of bleaching in the Red Sea during the following La Niña phase from 1998 to 2001, high summer SSTs are evident from satellite data (Figure 2), with the most extreme summer conditions documented in 2001. Following 2001, both cores showed a recovery of the seasonality in their trace element ratios. Remarkably, no clear signs of stress were observed in either core after this event, despite the fact that DHWs were higher in 2003 and 2005 than in 1998. The lack of clear signs of stress in the coral geochemistry points to either some degree of acclimatization in which exposure to stress *primes* corals to future stress

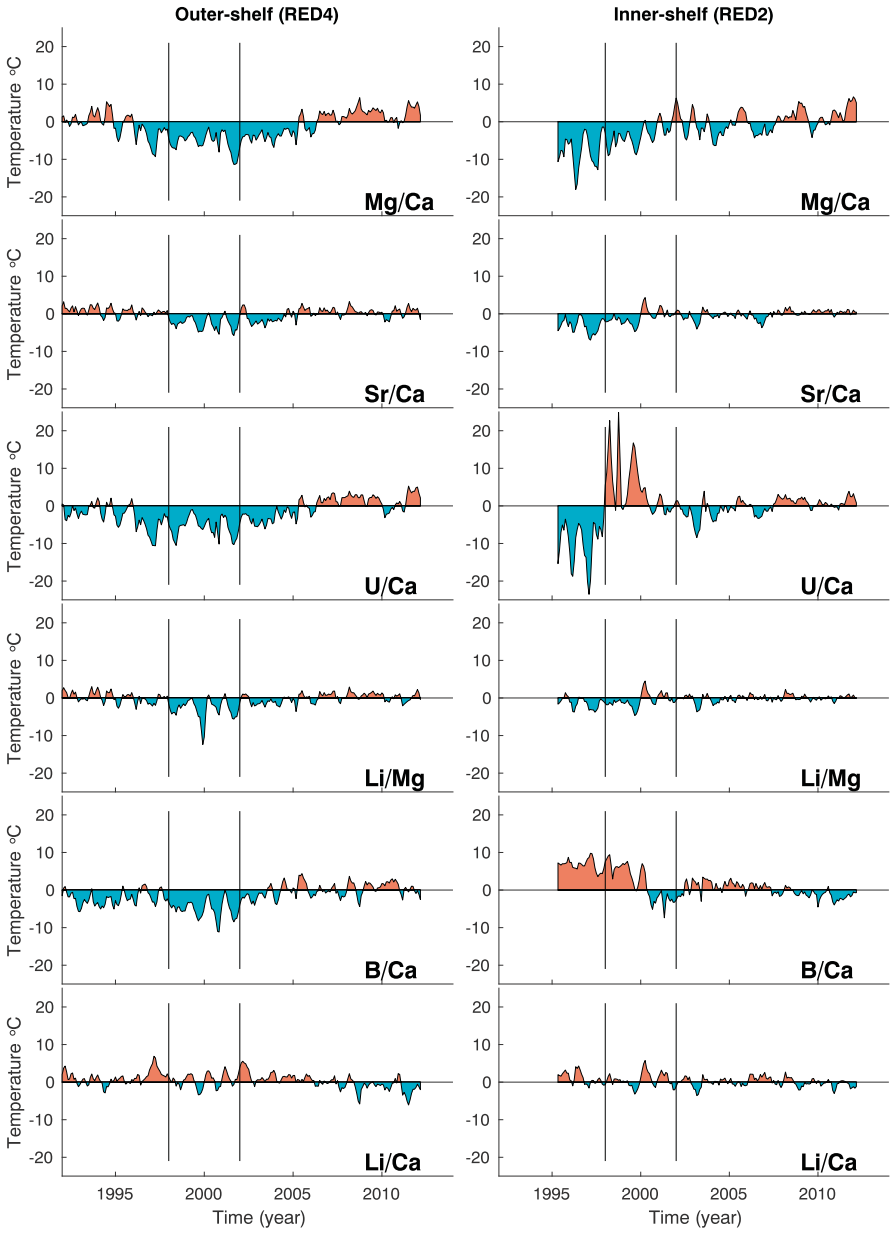

Figure 8. Residuals for the coral trace element ratios temperature reconstructions from inner-shelf and outer-shelf cores. Residuals were calculated as the difference between the temperatures calculated from each trace element and the AVHRR temperature data. The trace element temperatures were calculated using the calibration period of 2002 to 2012.

events, resulting in an increase in thermal tolerance (T. M. DeCarlo et al., 2019; Maynard et al., 2008). This could happen through either physiological adaptation, such as symbiont shuffling (Baker, 2003), bacterial restructuring (Ziegler et al., 2017), or regulation in gene expression (Kenkel & Matz, 2017)—in particular *front loading* (Barshis et al., 2013) whereby corals alter the relative levels of expression of housekeeping genes governing normal physiological maintenance and environmentally responsive genes that help protect the coral against unfavorable conditions (Dixon et al., 2018). If this was the case, *Porites* in the Red Sea respond differently from those in the equatorial Pacific that appear to bleach and recover during nearly every major ENSO event (Barkley et al., 2018).

Similarly, a major bleaching event was reported during the summer of 2010 in the central Red Sea with bleaching levels of 85% and 17% reported for *Porites* corals near Abu Shosha (inner shelf) and Shi'b

Nazar (outer shelf), respectively (Furby et al., 2013). Yet again the corals in this study showed no evidence of reduced growth or trace element disruption during that year, with only a minor disruption of some trace elements in 2009. The lack of a clear response in the geochemical record during 2010 could suggest that any acclimatization that may have taken place after the 1997–2001 event increased the resilience of these corals to subsequent thermal stress events on a long-term scale (~decadal). Alternatively, it could have been a combination of the strength and duration of the 1997–2001 ENSO event that caused the noticeable disruption in calcification and trace element incorporation that was not replicated during the milder 2010 La Niña event. For example, while the Coral Reef Watch virtual station that includes our study site (Al Madinah and Makkah) suggests 9 to 11 °C weeks of stress (Furby et al., 2013) in 2010, the AVHRR SST data for the grid point closest to our study sites showed low DHW (0.2 °C weeks) for 2010. Similarly, in 2015/2016 when bleaching was also reported in the region (Monroe et al., 2018), the site-specific DHWs were 0.1 °C weeks while the Coral Reef Watch station suggests >10 °C weeks. The discrepancy between the regional and local temperatures (Figure S5) impedes our ability to determine whether the lack of stress signal in the coral cores during 2010 was due to increased thermal tolerance or simply due to lower levels of thermal stress. Nevertheless, the direct observations of bleaching during 2010 (Furby et al., 2013) support the notion of an increase in thermal tolerance in the sampled corals. Although the present approach does not provide direct information whether a coral bleached or not, from a biomineralization perspective the data suggest that after the stress events of 1997–2001, these corals were not severely disrupted by subsequent stress events. This highlights the need to establish the differences in the geochemical signature between bleached and unbleached corals during bleaching events, in the context of their natural variability.

During stress events, a reduction in extension rate could result in a *bio-smoothing* of the trace element seasonal amplitude. The bio-smoothing model implies the progressive precipitation of aragonite over the thickness of the tissue layer attenuating the geochemical signal (Barnes et al., 1995; Taylor et al., 1993). If a coral reduces its rate of extension or increases the tissue thickness, then it would dampen the geochemical signal; therefore, the amplitude of the geochemical signal depends on the relationship between skeletal growth rate and mass accumulation within the tissue layer (Gagan et al., 2012). In this sense, a smoothing of 12 months (i.e., the tissue covers a full year of growth) and a constant rate of precipitation will remove all seasonality in the trace element ratios. The dampening of the seasonal signal could be further reduced by a decrease in sample resolution during periods of slow growth when samples are taken at fixed intervals. Nevertheless, D'Olivo and McCulloch (2017) identified trace element anomalies in a *Porites* coral core associated with a thermal stress event even when the sample resolution was adjusted to account for the reduction in extension rate. This bio-smoothing and reduction in resolution appears to, in general, explain the main changes observed in both coral records during the stress event, which was characterized by a reduction in seasonality but preservation of the relationship between different trace elements, independent of their different incorporation mechanisms. While most element ratios appear to maintain a constant relationship between each other (Figures 6 and 7), consistent with the smoothing model, U/Ca and B/Ca, particularly in the inner-shelf coral (RED2), showed a departure from the relationship observed with other trace elements between 1998 and 2001. In addition to the disruption of the geochemical seasonal signal, permanent and clear baseline changes were observed for all trace element ratios in the inner-shelf core following the 1998–2001 event. These overall changes in observed trace element ratios are generally consistent with an increase in Rayleigh fractionation during biomineralization (G. Gaetani & Cohen, 2006; G. A. Gaetani et al., 2011) resulting in a decrease in Sr/Ca, an increase in Mg/Ca, and no change in Li/Mg.

A *permanent* shift in the physiology of coral biomineralization was also manifest as a gradual increase in B/Ca over time; a shift that typically indicates a decrease in dissolved inorganic carbon (DIC) or carbonate ion concentration ($[CO_3^{2-}]$) in the calcifying fluid (T. M. DeCarlo et al., 2018; Holcomb et al., 2016). Similarly, U/Ca, considered to be influenced by $[CO_3^{2-}]$ (T. M. DeCarlo et al., 2015), showed a significant change in the inner-shelf coral. However, B/Ca and U/Ca show opposing behaviors after 1998–2001, that is, ~20% increase in B/Ca and ~15% reduction in U/Ca, indicative of further complications to the incorporation of these elemental ratios that are beyond the scope of this paper to determine. The divergence between the B/Ca and U/Ca signals precludes us from conclusively establishing the nature of the change in $[CO_3^{2-}]$ or DIC but is nevertheless indicative of a permanent change in the coral biomineralization process. In contrast, no clear changes in the relationship between different trace elements were observed for the outer-shelf

core. Furthermore, while the change point analysis reveals that discrete shifts in most trace element ratios occurred between 1996 and 1998, these same ratios appear to return to predisturbance levels between 2002 and 2005 with much smaller changes (<5%) for both B/Ca and U/Ca data when compared to the inner-shelf coral data. This suggests that compared to the inner-shelf coral, no significant change in the DIC available for calcification occurred in outer-shelf coral. Differences in the response between the two cores could be related to lower levels of stress during bleaching events due to oceanographic differences or to different levels of acclimatization. Species-specific effects could also affect the incorporation of trace elements (D'Olivo et al., 2018), and possibly the response and recovery following thermal stress events, further complicating the comparisons between the two cores and highlighting the need for further studies. While results from the outer-shelf coral are less conclusive, the response from the inner-shelf coral suggests that stress-induced changes could have a relatively long term impact that potentially increases thermal tolerance of some corals.

5. Conclusions

Our data reveal how extreme thermal stress events can alter the incorporation of multiple trace elements into coral aragonite skeletons. Trace elements are known to be influenced by the physiological controls on biomineralization under normal conditions, but they are even more sensitive to alterations of coral physiology during periods of prolonged stress—such as when the zooxanthellae-coral host relationship is compromised. These stress events appear capable of producing permanent or long-term physiological changes that affect the incorporation of the trace elements into the skeleton, thereby compromising the extrapolation of these paleothermometers across periods of elevated physiological stress. The lack of signs of stress in the *Porites* corals studied following documented bleaching events (e.g., 2010) suggests that some level of acclimatization might have occurred following earlier stress events (~1997–2001); however, the underlying mechanisms remain elusive at this point. Nevertheless, the high levels of mortality observed in 2010 clearly demonstrate that this acclimatization is limited in its overall effect as most coral species remain highly vulnerable to increasingly more extreme marine heat waves.

Acknowledgments
We would like to acknowledge the team at KAUST for their support, knowledge, and hospitality while the coral cores were being retrieved. With special thanks to Anna Roik for her input in this paper. We thank the technical staff of AGFIOR, Kai Rankenburg and Anne-Marin Nisumaa Comeau for their laboratory expertise. This research was supported by King Abdullah University of Science and Technology (KAUST) and by funding provided by an ARC Laureate Fellowship (LF120100049) awarded to Professor Malcolm McCulloch and the ARC Centre of Excellence for Coral Reef Studies (CE140100020). All the geochemical data generated are available at https://doi.pangaea.de/10.1594/PANGAEA.901186.

References

Alibert, C., & McCulloch, M. T. (1997). Strontium/calcium ratios in modern *Porites* corals from the Great Barrier Reef as a proxy for sea surface temperature: Calibration of the thermometer and monitoring of ENSO. *Paleoceanography*, *12*(3), 345–363. https://doi.org/10.1029/97pa00318

Baker, A. C. (2003). Flexibility and specificity in coral-algal symbiosis: Diversity, ecology, and biogeography of *Symbiodinium*. *Annual Review of Ecology Evolution and Systematics*, *34*(1), 661–689. https://doi.org/10.1146/annurev.ecolsys.34.011802.132417

Barkley, H. C., Cohen, A. L., Mollica, N. R., Brainard, R. E., Rivera, H. E., DeCarlo, T. M., et al. (2018). Repeat bleaching of a central Pacific coral reef over the past six decades (1960–2016). *Communications Biology*, *1*(1), 177. https://doi.org/10.1038/s42003-018-0183-7

Barnes, D. J., & Lough, J. M. (1993). On the nature and causes of density banding in massive coral skeletons. *Journal of Experimental Marine Biology and Ecology*, *167*(1), 91–108. https://doi.org/10.1016/0022-0981(93)90186-R

Barnes, D. J., Taylor, R. B., & Lough, J. M. (1995). On the inclusion of trace materials into massive coral skeletons.2. Distortions in skeletal records of annual climate cycles due to growth processes. *Journal of Experimental Marine Biology and Ecology*, *194*(2), 251–275. https://doi.org/10.1016/0022-0981(95)00091-7

Barshis, D. J., Ladner, J. T., Oliver, T. A., Seneca, F. O., Traylor-Knowles, N., & Palumbi, S. R. (2013). Genomic basis for coral resilience to climate change. *Proc Natl Acad Sci U S A*, *110*(4), 1387–1392. https://doi.org/10.1073/pnas.1210224110

Beck, J. W., Edwards, R. L., Ito, E., Taylor, F. W., Recy, J., Rougerie, F., et al. (1992). Sea-surface temperature from coral skeletal strontium/calcium ratios. *Science*, *257*(5070), 644–647. https://doi.org/10.1126/science.257.5070.644

Cantin, N. E., Cohen, A. L., Karnauskas, K. B., Tarrant, A. M., & McCorkle, D. C. (2010). Ocean warming slows coral growth in the central Red Sea. *Science*, *329*(5989), 322–325. https://doi.org/10.1126/science.1190182

Cantin, N. E., & Lough, J. M. (2014). Surviving coral bleaching events: Porites growth anomalies on the Great Barrier Reef. *PLoS One*, *9*(2), e88720. https://doi.org/10.1371/journal.pone.0088720

Case, D. H., Robinson, L. F., Auro, M. E., & Gagnon, A. C. (2010). Environmental and biological controls on Mg and Li in deep-sea scleractinian corals. *Earth and Planetary Science Letters*, *300*(3-4), 215–225. https://doi.org/10.1016/j.epsl.2010.09.029

Clarke, H., D'Olivo, J. P., Falter, J., Zinke, J., Lowe, R., & McCulloch, M. (2017). Differential response of corals to regional mass-warming events as evident from skeletal Sr/Ca and Mg/Ca ratios. *Geochemistry Geophysics Geosystems*, *18*, 1794–1809. https://doi.org/10.1002/2016GC006788

Cohen, A. L., Owens, K. E., Layne, G. D., & Shimizu, N. (2002). The effect of algal symbionts on the accuracy of Sr/Ca paleotemperatures from coral. *Science*, *296*(5566), 331–333. https://doi.org/10.1126/science.1069330

Davis, K. A., Lentz, S. J., Pineda, J., Farrar, J. T., Starczak, V. R., & Churchill, J. H. (2011). Observations of the thermal environment on Red Sea platform reefs: A heat budget analysis. *Coral Reefs*, *30*(S1), 25–36. https://doi.org/10.1007/s00338-011-0740-8

DeCarlo, T. M., & Cohen, A. L. (2017). Dissepiments, density bands and signatures of thermal stress in *Porites* skeletons. *Coral Reefs*, *36*(3), 749–761. https://doi.org/10.1007/s00338-017-1566-9

DeCarlo, T. M., Gaetani, G. A., Cohen, A. L., Foster, G. L., Alpert, A. E., & Stewart, J. A. (2016). Coral Sr-U thermometry. *Paleoceanography*, *31*, 626–638. https://doi.org/10.1002/2015pa002908

DeCarlo, T. M., Gaetani, G. A., Holcomb, M., & Cohen, A. L. (2015). Experimental determination of factors controlling U/Ca of aragonite precipitated from seawater: Implications for interpreting coral skeleton. *Geochimica et Cosmochimica Acta*, *162*, 151–165. https://doi.org/10.1016/j.gca.2015.04.016

DeCarlo, T. M., Harrison, H. B., Gajdzik, L., Alaguarda, D., Rodolfo-Metalpa, R., D'Olivo, J., et al. (2019). Acclimatization of massive reef-building corals to consecutive heatwaves. *Proceedings of the Royal Society B: Biological Sciences*, *286*(1898). https://doi.org/10.1098/rspb.2019.0235

DeCarlo, T. M., Holcomb, M., & McCulloch, M. T. (2018). Reviews and syntheses: Revisiting the boron systematics of aragonite and their application to coral calcification. *Biogeosciences*, *15*(9), 2819–2834. https://doi.org/10.5194/bg-15-2819-2018

DeLong, K. L., Quinn, T. M., & Taylor, F. W. (2007). Reconstructing twentieth-century sea surface temperature variability in the southwest Pacific: A replication study using multiple coral Sr/Ca records from New Caledonia. *Paleoceanography*, *22*, PA4212. https://doi.org/10.1029/2007PA001444

DeLong, K. L., Quinn, T. M., Taylor, F. W., Shen, C.-C., & Lin, K. (2013). Improving coral-base paleoclimate reconstructions by replicating 350 years of coral Sr/Ca variations. *Palaeogeography, Palaeoclimatology, Palaeoecology*, *373*, 6–24. https://doi.org/10.1016/j.palaeo.2012.08.019

DeVantier, L., Tourak, E., & Al-Shaikh, K. (2000). Coral bleaching in the central-northern Saudi Arabian Red Sea, August-September 1998. Paper presented at the Proceedings of the International Workshop on the Extent and Impact of Coral Bleaching in the Arabian Region.

Dixon, G., Liao, Y., Bay, L. K., & Matz, M. V. (2018). Role of gene body methylation in acclimatization and adaptation in a basal metazoan. *Proceeding National Academy of Science.*, *115*(52), 13,342–13,346. https://doi.org/10.1073/pnas.1813749115

D'Olivo, J. P., & McCulloch, M. T. (2017). Response of coral calcification and calcifying fluid composition to thermally induced bleaching stress. *Scientific Reports*, *7*(1), 2207. https://doi.org/10.1038/s41598-017-02306-x

D'Olivo, J. P., McCulloch, M. T., & Judd, K. (2013). Long-term records of coral calcification across the central Great Barrier Reef: Assessing the impacts of river runoff and climate change. *Coral Reefs*, *32*(4), 999–1012. https://doi.org/10.1007/s00338-013-1071-8

D'Olivo, J. P., Sinclair, D. J., Rankenburg, K., & McCulloch, M. T. (2018). A universal multi-trace element calibration for reconstructing sea surface temperatures from long-lived Porites corals: Removing 'vital-effects. *Geochimica et Cosmochimica Acta*, *239*, 109–135. https://doi.org/10.1016/j.gca.2018.07.035

Felis, T., Patzold, J., Loya, Y., Fine, M., Nawar, A. H., & Wefer, G. (2000). A coral oxygen isotope record from the northern Red Sea documenting NAO, ENSO, and North Pacific teleconnections on Middle East climate variability since the year 1750. *Paleoceanography*, *15*(6), 679–694. https://doi.org/10.1029/1999pa000477

Felis, T., Suzuki, A., Kuhnert, H., Dima, M., Lohmann, G., & Kawahata, H. (2009). Subtropical coral reveals abrupt early-twentieth-century freshening in the western North Pacific Ocean. *Geology*, *37*(6), 527–530. https://doi.org/10.1130/g25581a.1

Finch, A. A., & Allison, N. (2008). Mg structural state in coral aragonite and implications for the paleoenvironmental proxy. *Geophysical Research Letters*, *35*, L08704. https://doi.org/10.1029/2008GL033543

Fowell, S. E., Sandford, K., Stewart, J. A., Castillo, K. D., Ries, J. B., & Foster, G. L. (2016). Intrareef variations in Li/Mg and Sr/Ca sea surface temperature proxies in the Caribbean reef-building coral Siderastrea siderea. *Paleoceanography*, *31*, 1315–1329. https://doi.org/10.1002/2016PA002968

Furby, K. A., Bouwmeester, J., & Berumen, M. L. (2013). Susceptibility of central Red Sea corals during a major bleaching event. *Coral Reefs*, *32*(2), 505–513. https://doi.org/10.1007/s00338-012-0998-5

Gaetani, G., & Cohen, A. (2006). Element partitioning during precipitation of aragonite from seawater: A framework for understanding paleoproxies. *Geochimica et Cosmochimica Acta*, *70*(18), 4617–4634. https://doi.org/10.1016/j.gca.2006.07.008

Gaetani, G. A., Cohen, A. L., Wang, Z., & Crusius, J. (2011). Rayleigh-based, multi-element coral thermometry: A biomineralization approach to developing climate proxies. *Geochimica et Cosmochimica Acta*, *75*(7), 1920–1932. https://doi.org/10.1016/j.gca.2011.01.010

Gagan, M. K., Dunbar, G. B., & Suzuki, A. (2012). The effect of skeletal mass accumulation in *Porites* on coral Sr/Ca and δ18O paleothermometry. *Paleoceanography*, *27*, PA1203. https://doi.org/10.1029/2011PA002215

Gintert, B. E., Manzello, D. P., Enochs, I. C., Kolodziej, G., Carlton, R., Gleason, A. C. R., & Gracias, N. (2018). Marked annual coral bleaching resilience of an inshore patch reef in the Florida Keys: A nugget of hope, aberrance, or last man standing? *Coral Reefs*, *37*(2), 533–547. https://doi.org/10.1007/s00338-018-1678-x

Goreau, T. J. (1977). Coral skeletal chemistry—Physiological and environmental regulation of stable isotopes and trace-metals in Montastrea-Annularis. *Proceedings of the Royal Society Series B-Biological Sciences*, *196*(1124), 291–315. https://doi.org/10.1098/rspb.1977.0042

Guest, J. R., Baird, A. H., Maynard, J. A., Muttaqin, E., Edwards, A. J., Campbell, S. J., et al. (2012). Contrasting patterns of coral bleaching susceptibility in 2010 suggest an adaptive response to thermal stress. *PLoS One*, *7*(3). https://doi.org/10.1371/journal.pone.0033353

Hathorne, E. C., Felis, T., Suzuki, A., Kawahata, H., & Cabioch, G. (2013). Lithium in the aragonite skeletons of massive *Porites* corals: A new tool to reconstruct tropical sea surface temperatures. *Paleoceanography*, *28*, 143–152. https://doi.org/10.1029/2012PA002311

Hathorne, E. C., Gagnon, A., Felis, T., Adkins, J., Asami, R., Boer, W., et al. (2013). Interlaboratory study for coral Sr/Ca and other element/Ca ratio measurements. *Geochemistry, Geophysics, Geosystems*, *14*, 3730–3750. https://doi.org/10.1002/ggge.20230

Hetzinger, S., Pfeiffer, M., Dullo, W. C., Zinke, J., & Garbe-Schonberg, D. (2016). A change in coral extension rates and stable isotopes after El Niño-induced coral bleaching and regional stress events. *Scientific Reports*, *6*(1), 32879. https://doi.org/10.1038/srep32879

Holcomb, M., DeCarlo, T. M., Gaetani, G. A., & McCulloch, M. (2016). Factors affecting B/Ca ratios in synthetic aragonite. *Chemical Geology*, *437*, 67–76. https://doi.org/10.1016/j.chemgeo.2016.05.007

Holcomb, M., DeCarlo, T. M., Schoepf, V., Dissard, D., Tanaka, K., & McCulloch, M. (2015). Cleaning and pre-treatment procedures for biogenic and synthetic calcium carbonate powders for determination of elemental and boron isotopic compositions. *Chemical Geology*, *398*, 11–21. https://doi.org/10.1016/j.chemgeo.2015.01.019

Ionita, M., Felis, T., Lohmann, G., Rimbu, N., & Patzold, J. (2014). Distinct modes of East Asian winter monsoon documented by a southern Red Sea coral record. *Journal of Geophysical Research: Oceans*, *119*, 1517–1533. https://doi.org/10.1002/2013JC009203

Isdale, P. J. (1984). Fluorescent bands in massive corals record centuries of coastal rainfall. *Nature*, *310*(5978), 578–579. https://doi.org/10.1038/310578a0

Kenkel, C. D., & Matz, M. V. (2017). Gene expression plasticity as a mechanism of coral adaptation to a variable environment. *Nature Ecology & Evolution*, *1*(1). https://doi.org/10.1038/s41559-016-0014

Klein, R., Tudhope, A. W., Chilcott, C. P., Pätzold, J., Abdulkarim, Z., Fine, M., et al. (1997). Evaluating southern Red Sea corals as a proxy record for the Asian monsoon. *Earth and Planetary Science Letters*, *148*(1-2), 381–394. https://doi.org/10.1016/S0012-821x(97)00021-6

Liu, G., Rauenzahn, J. L., Heron, S. F., Eakin, C. M., Skirving, W. J., Christensen, T. R. L., & Strong, A. E. L., J. (2013). NOAA Coral Reef Watch 50 km satellite sea surface temperature-based decision support system for coral bleaching management. Retrieved from NOAA/NESDIS: College Park, MD, USA:

Liu, W., Huang, B., Thorne, P. W., Banzon, V. F., Zhang, H. M., Freeman, E., et al. (2015). Extended reconstructed sea surface temperature version 4 (ERSST.v4): Part II. Parametric and structural uncertainty estimations. *Journal of Climate*, *28*(3), 931–951. https://doi.org/10.1175/Jcli-D-14-00007.1

Marchitto, T. M., Bryan, S. P., Doss, W., McCulloch, M. T., & Montagna, P. (2018). A simple biomineralization model to explain Li, Mg, and Sr incorporation into aragonitic foraminifera and corals. *Earth and Planetary Science Letters*, *481*, 20–29. https://doi.org/10.1016/j.epsl.2017.10.022

Marriott, C. S., Henderson, G. M., Belshaw, N. S., & Tudhope, A. W. (2004). Temperature dependence of delta Li-7, delta Ca-44 and Li/Ca during growth of calcium carbonate. *Earth and Planetary Science Letters*, *222*(2), 615–624. https://doi.org/10.1016/j.epsl.2004.02.031

Marshall, J. F., & McCulloch, M. T. (2002). An assessment of the Sr/Ca ratio in shallow water hermatypic corals as a proxy for sea surface temperature. *Geochimica et Cosmochimica Acta*, *66*(18), 3263–3280. https://doi.org/10.1016/s0016-7037(02)00926-2

Maynard, J. A., Anthony, K. R. N., Marshall, P. A., & Masiri, I. (2008). Major bleaching events can lead to increased thermal tolerance in corals. *Marine Biology*, *155*(2), 173–182. https://doi.org/10.1007/s00227-008-1015-y

McCulloch, M. T., Gagan, M. K., Mortimer, G. E., Chivas, A. R., & Isdale, P. J. (1994). A high-resolution Sr/Ca and δ18O coral record from the Great Barrier Reef, Australia, and the 1982–1983 El Niño. *Geochimica et Cosmochimica Acta*, *58*(12), 2747–2754. https://doi.org/10.1016/0016-7037(94)90142-2

McCulloch, M. T., & Mortimer, G. E. (2008). Applications of the U-238-Th-230 decay series to dating of fossil and modern corals using MC-ICPMS. *Australian Journal of Earth Sciences*, *55*(6-7), 955–965. https://doi.org/10.1080/08120090802097435

Monismith, S. G., Genin, A., Reidenbach, M. A., Yahel, G., & Koseff, J. R. (2006). Thermally driven exchanges between a coral reef and the adjoining ocean. *Journal of Physical Oceanography*, *36*(7), 1332–1347. https://doi.org/10.1175/Jpo2916.1

Monroe, A. A., Ziegler, M., Roik, A., Röthig, T., Hardenstine, R. S., Emms, M. A., et al. (2018). In situ observations of coral bleaching in the central Saudi Arabian Red Sea during the 2015/2016 global coral bleaching event. *PLoS One*, *13*(4), e0195814. https://doi.org/10.1371/journal.pone.0195814

Montagna, P., McCulloch, M., Douville, E., López Correa, M., Trotter, J., Rodolfo-Metalpa, R., et al. (2014). Li/Mg systematics in scleractinian corals: Calibration of the thermometer. *Geochimica et Cosmochimica Acta*, *132*, 288–310. https://doi.org/10.1016/j.gca.2014.02.005

Montagna, P., McCulloch, M., Taviani, M., Trotter, J., Silenzi, S., & Mazzoli, C. (2009). An improved sampling method for coral P/Ca as a nutrient proxy. *Geochimica et Cosmochimica Acta*, *73*(13), A895–A895.

Moreau, M., Correge, T., Dassie, E. P., & Le Cornec, F. (2015). Evidence for the non-influence of salinity variability on the Porites coral Sr/Ca palaeothermometer. *Climate of the Past*, *11*(3), 523–532. https://doi.org/10.5194/cp-11-523-2015

National Oceanic and Atmospheric Administration, C. R. W. (2000). Satellite coral bleaching degree heating week product.

Nurhati, I. S., Cobb, K. M., Charles, C. D., & Dunbar, R. B. (2009). Late 20th century warming and freshening in the central tropical Pacific. *Geophysical Research Letters*, *36*, L21606. https://doi.org/10.1029/2009GL040270

Osman, E. O., Smith, D. J., Ziegler, M., Kürten, B., Conrad, C., el-Haddad, K. M., et al. (2018). Thermal refugia against coral bleaching throughout the northern Red Sea. *Global Change Biology*, *24*(2), E474–E484. https://doi.org/10.1111/gcb.13895

Paillard, D., Labeyrie, L., & Yiou, P. (1996). Macintosh program performs time-series analysis. *Eos, Transactions American Geophysical Union*, *77*(39), 379–379. https://doi.org/10.1029/96eo00259

Palmer, C. V. (2018). Immunity and the coral crisis. *Commun Biol*, *1*(1), 91. https://doi.org/10.1038/s42003-018-0097-4

Pratchett, M. S., McCowan, D., Maynard, J. A., & Heron, S. F. (2013). Changes in bleaching susceptibility among corals subject to ocean warming and recurrent bleaching in Moorea, French Polynesia. *PLoS One*, *8*(7), e70443. https://doi.org/10.1371/journal.pone.0070443

Putnam, H. M., Barott, K. L., Ainsworth, T. D., & Gates, R. D. (2017). The vulnerability and resilience of reef-building corals. *Current Biology*, *27*(11), R528–R540. https://doi.org/10.1016/j.cub.2017.04.047

Rasul, N. M. A., Stewart, I. C. F., & Nawab, Z. A. (2015). Introduction to the Red Sea: Its origin, structure, and environment. Red Sea: The Formation, Morphology, Oceanography and Environment of a Young Ocean Basin, 1-28. doi:https://doi.org/10.1007/978-3-662-45201-1_1

Reynolds, R. W., Smith, T. M., Liu, C., Chelton, D. B., Casey, K. S., & Schlax, M. G. (2007). Daily high-resolution-blended analyses for sea surface temperature. *Journal of Climate*, *20*(22), 5473–5496. https://doi.org/10.1175/2007jcli1824.1

Rimbu, N., Lohmann, G., Felis, T., & Patzold, J. (2001). Arctic oscillation signature in a Red Sea coral. *Geophysical Research Letters*, *28*(15), 2959–2962. https://doi.org/10.1029/2001gl013083

Roik, A., Rothig, T., Roder, C., Muller, P. J., & Voolstra, C. R. (2015). Captive rearing of the deep-sea coral *Eguchipsammia fistula* from the Red Sea demonstrates remarkable physiological plasticity. *PeerJ*, *3*, e734. https://doi.org/10.7717/peerj.734

Roik, A., Rothig, T., Roder, C., Ziegler, M., Kremb, S. G., & Voolstra, C. R. (2016). Year-long monitoring of physico-chemical and biological variables provide a comparative baseline of coral reef functioning in the central Red Sea. *PLoS One*, *11*(11), e0163939. https://doi.org/10.1371/journal.pone.0163939

Rollion-Bard, C., & Blamart, D. (2015). Possible controls on Li, Na, and Mg incorporation into aragonite coral skeletons. *Chemical Geology*, *396*, 98–111. https://doi.org/10.1016/j.chemgeo.2014.12.011

Sagar, N., Hetzinger, S., Pfeiffer, M., Ahmad, S. M., Dullo, W. C., & Garbe-Schonberg, D. (2016). High-resolution Sr/Ca ratios in a *Porites lutea* coral from Lakshadweep Archipelago, southeast Arabian Sea: An example from a region experiencing steady rise in the reef temperature. *Journal of Geophysical Research: Oceans*, *121*, 252–266. https://doi.org/10.1002/2015jc010821

Schoepf, V., Stat, M., Falter, J. L., & McCulloch, M. T. (2015). Limits to the thermal tolerance of corals adapted to a highly fluctuating, naturally extreme temperature environment. *Scientific Reports*, *5*(1), 17,639. https://doi.org/10.1038/srep17639

Sinclair, D. J. (2005). Correlated trace element "vital effects" in tropical corals: A new geochemical tool for probing biomineralization. *Geochimica et Cosmochimica Acta*, *69*(13), 3265–3284. https://doi.org/10.1016/j.gca.2005.02.030

Sinclair, D. J., & Risk, M. J. (2006). A numerical model of trace-element coprecipitation in a physicochemical calcification system: Application to coral biomineralization and trace-element 'vital effects'. *Geochimica et Cosmochimica Acta*, *70*(15), 3855–3868. https://doi.org/10.1016/j.gca.2006.05.019

Stocker, T. F., Qin, D., Plattner, G., Tignor, M., Allen, S. K., Boschung, J., Nauels, A., Xia, Y., Bex, V., Midgley, P. (2013). IPCC 2013: The Physical Science Basis. Contribution of Working Group I to the Fifth Assessment Report of the Intergovernmental Panel on Climate Change. Retrieved from

Suzuki, A., Gagan, M. K., Fabricius, K., Isdale, P. J., Yukino, I., & Kawahata, H. (2003). Skeletal isotope microprofiles of growth perturbations in *Porites* corals during the 1997-1998 mass bleaching event. *Coral Reefs*, *22*(4), 357–369. https://doi.org/10.1007/s00338-003-0323-4

Tanaka, K., Holcomb, M., Takahashi, A., Kurihara, H., Asami, R., Shinjo, R., et al. (2015). Response of *Acropora digitifera* to ocean acidification: Constraints from $\delta^{11}B$, Sr, Mg, and Ba compositions of aragonitic skeletons cultured under variable seawater pH. *Coral Reefs*, *34*(4), 1139–1149. https://doi.org/10.1007/s00338-015-1319-6

Taylor, R. B., Barnes, D. J., & Lough, J. M. (1993). Simple-models of density band formation in massive corals. *Journal of Experimental Marine Biology and Ecology*, *167*(1), 109–125. https://doi.org/10.1016/0022-0981(93)90187-S

Veron, J. E. N. (2000). *Corals of the world*. Townsville, Australia: Australian Institute of Marine Science.

Watson, E. B. (1996). Surface enrichment and trace-element uptake during crystal growth. *Geochimica et Cosmochimica Acta*, *60*(24), 5013–5020. https://doi.org/10.1016/S0016-7037(96)00299-2

Watson, E. B. (2004). A conceptual model for near-surface kinetic controls on the trace-element and stable isotope composition of abiogenic calcite crystals. *Geochimica et Cosmochimica Acta*, *68*(7), 1473–1488. https://doi.org/10.1016/j.gca.2003.10.003

Wilkinson, C. (2000). *Status of coral reefs of the world: 2000*. Australia: Townsville.

Ziegler, M., Seneca, F. O., Yum, L. K., Palumbi, S. R., & Voolstra, C. R. (2017). Bacterial community dynamics are linked to patterns of coral heat tolerance. *Nature Communications*, *8*(1). https://doi.org/10.1038/ncomms14213

Zinke, J., D'Olivo, J. P., Gey, C. J., McCulloch, M. T., Bruggemann, J. H., Lough, J. M., & Guillaume, M. M. (2019). Multi-trace-element sea surface temperature coral reconstruction for the southern Mozambique Channel reveals teleconnections with the tropical Atlantic. *Biogeosciences*, *16*(3), 695–712. https://doi.org/10.5194/bg-16-695-2019

Zinke, J., Hoell, A., Lough, J. M., Feng, M., Kuret, A. J., Clarke, H., et al. (2015). Coral record of southeast Indian Ocean marine heatwaves with intensified Western Pacific temperature gradient. *Nature Communications*, *6*(1), 8562. https://doi.org/10.1038/ncomms9562